

NDHU-TH-97-01  
UDHEP-11-97  
November 1997

**Chiral Symmetry Breaking in a Uniform  
External Magnetic Field II.  
Symmetry Restoration at High Temperatures  
and Chemical Potentials**

**D.-S. Lee<sup>(a)</sup>, C. N. Leung<sup>(b)</sup> and Y. J. Ng<sup>(c)</sup>**

*(a) Department of Physics, National Dong Hwa University,  
Shoufeng, Hualien 974, Taiwan*

*(b) Department of Physics and Astronomy, University of Delaware,  
Newark, DE 19716*

*(c) Institute of Field Physics, Department of Physics and Astronomy,  
University of North Carolina, Chapel Hill, NC 27599*

**Abstract**

Chiral symmetry is dynamically broken in quenched, ladder QED at weak gauge couplings when an external magnetic field is present. In this paper, we show that chiral symmetry is restored above a critical chemical potential and the corresponding phase transition is of first order. In contrast, the chiral symmetry restoration at high temperatures (and at zero chemical potential) is a second order phase transition.

Do external fields affect the symmetry properties of the vacuum? [1] The answer is yes; in particular, it was found that, in the quenched, ladder approximation of QED, chiral symmetry is dynamically broken at weak gauge couplings when a uniform magnetic field is present [2,3]. Subsequently, in a more detailed exposition [4], we show that chiral symmetry is restored above a critical temperature which is of the order of  $m_0$ , the dynamical fermion mass generated at zero temperature and zero chemical potential (see also [5]). In this paper, we consider the effects of a chemical potential on the chiral symmetry breaking in QED induced by a magnetic field. We find that chiral symmetry is restored above a critical chemical potential  $\mu_c$  which is proportional to  $m_0$  with the proportional factor a function of the gauge coupling constant. We also find that the dynamical fermion mass  $m_\mu$  generated at nonzero chemical potential increases from  $m_0$  as the chemical potential  $\mu$  is increased from zero toward  $\mu_c$  and exhibits a discontinuous jump to  $m_\mu = 0$  when the critical chemical potential is crossed. The order parameter for the phase transition, the chiral condensate  $\langle\bar{\psi}\psi\rangle$ , has the similar discontinuous behavior at  $\mu_c$ . This indicates that the corresponding phase transition is of first order. For comparison, we study the nature of the chiral phase transition at high temperature but with zero chemical potential. This phase transition is of second order since the dynamical fermion thermal mass  $m_T$  as well as the corresponding chiral condensate approach zero continuously as the temperature approaches the critical temperature from below.

Unless otherwise noted, all notations are the same as those in Ref. [4], hereafter referred to as I.

The effects of a chemical potential  $\mu$  can be incorporated into the study of chiral symmetry breaking in an external magnetic field at nonzero temperature [4] by making the substitution [6]:

$$p_0 \rightarrow i\pi T(2l + 1) - \mu, \quad l = 0, \pm 1, \pm 2, \dots \quad (1)$$

for the fermion energy. The thermal photon propagator remains unchanged. One can easily show that the presence of a chemical potential does not modify the orthogonality

and completeness conditions [7] of the basis eigenfunctions used in our formalism. It is then straightforward to follow the procedures described in I to obtain the gap equation for nonzero temperature and nonzero chemical potential:

$$1 \simeq \frac{2\alpha}{\pi} T |eH| \int_{-\infty}^{\infty} dq_3 \int_0^{\infty} d\hat{q}_\perp^2 e^{-\hat{q}_\perp^2} \sum_l \frac{1}{Q_2^2 + 4\pi^2 T^2 l^2} \frac{1}{Q_1^2 + [\pi T(2l-1) - i\mu]^2} \quad (2)$$

where  $Q_1^2 \equiv q_3^2 + m^2(T, \mu)$ ,  $Q_2^2 \equiv q_3^2 + 2|eH|\hat{q}_\perp^2$ , and  $m(T, \mu)$  is the infrared dynamical fermion mass as a function of both the temperature and the chemical potential.

We sum over  $l$  in Eq.(2) using the Poisson sum formula. The gap equation now reads

$$\begin{aligned} 1 \simeq & \frac{\alpha}{2\pi} |eH| \int_{-\infty}^{\infty} dq_3 \int_0^{\infty} d\hat{q}_\perp^2 \frac{e^{-\hat{q}_\perp^2}}{Q_1 Q_2} \\ & \cdot \left\{ Q_1 \coth\left(\frac{Q_2}{2T}\right) \left[ \frac{1}{Q_1^2 - (Q_2 + \mu - i\pi T)^2} + \frac{1}{Q_1^2 - (Q_2 - \mu + i\pi T)^2} \right] \right. \\ & \left. + Q_2 \left[ \frac{\tanh(\frac{Q_1+\mu}{2T})}{Q_2^2 - (Q_1 + \mu - i\pi T)^2} + \frac{\tanh(\frac{Q_1-\mu}{2T})}{Q_2^2 - (Q_1 - \mu + i\pi T)^2} \right] \right\}. \end{aligned} \quad (3)$$

In the  $\mu = 0$  limit, this equation reduces to the nonzero temperature gap equation obtained in I [8].

Following the procedure described in Appendix B of I, one can obtain the chiral condensate at nonzero temperature and nonzero chemical potential as

$$\langle \bar{\psi} \psi \rangle_{T\mu} \simeq - \frac{2|eH|}{\pi^2} T \sum_l \int_0^{\sqrt{|eH|}} dp_3 \frac{m(T, \mu)}{[(2l+1)\pi T + i\mu]^2 + p_3^2 + m^2(T, \mu)}, \quad (4)$$

where we have cut off the momentum integral at  $\sqrt{|eH|}$  (because the dynamical fermion mass would be vanishingly small at momenta above  $\sqrt{|eH|}$ ) and ignored the momentum dependence in  $m$ . The sum can again be evaluated by means of the Poisson sum formula to yield

$$\langle \bar{\psi} \psi \rangle_{T\mu} \simeq - \frac{|eH|}{\pi^2} m \int_0^{\sqrt{|eH|}} \frac{dp_3}{\sqrt{p_3^2 + m^2}} S_{T\mu}, \quad (5)$$

where

$$S_{T\mu} = \frac{1}{1 + e^{-\frac{\sqrt{p_3^2 + m^2} + |\mu|}{T}}} - \frac{\theta(|\mu| - \sqrt{p_3^2 + m^2})}{1 + e^{-\frac{|\mu| - \sqrt{p_3^2 + m^2}}{T}}} - \theta(\sqrt{p_3^2 + m^2} - |\mu|) \left[ 1 - \frac{1}{1 + e^{-\frac{\sqrt{p_3^2 + m^2} - |\mu|}{T}}} \right]. \quad (6)$$

In the limit  $T = \mu = 0$ ,  $S_{00}$  equals 1 and we get ( $m_0 \equiv m(0, 0)$ )

$$\begin{aligned}\langle \bar{\psi} \psi \rangle_{00} &\simeq -\frac{|eH|}{\pi^2} m_0 \int_0^{\sqrt{|eH|}} \frac{dp_3}{\sqrt{p_3^2 + m_0^2}} \\ &\simeq -\frac{|eH|}{2\pi^2} m_0 \ln \left( \frac{|eH|}{m_0^2} \right),\end{aligned}\quad (7)$$

in agreement with the result given by Eq.(B4) in I.

To isolate the effects of the chemical potential on chiral symmetry breaking in the presence of an external magnetic field, we now consider the  $T = 0$  limit of the above gap equation. We note the following simplification in this limit:

$$\begin{aligned}\coth \left( \frac{Q_2}{2T} \right) &\rightarrow 1, \\ \tanh \left( \frac{Q_1 + \mu}{2T} \right) &\rightarrow \theta(\mu) + \theta(-\mu) [\theta(Q_1 + \mu) - \theta(-\mu - Q_1)], \\ \tanh \left( \frac{Q_1 - \mu}{2T} \right) &\rightarrow \theta(\mu) [\theta(Q_1 - \mu) - \theta(\mu - Q_1)] + \theta(-\mu).\end{aligned}$$

Eq.(3) is then reduced to

$$\begin{aligned}1 &\simeq \frac{\alpha}{2\pi} |eH| \int_{-\infty}^{\infty} dq_3 \int_0^{\infty} d\hat{q}_\perp^2 \frac{e^{-\hat{q}_\perp^2}}{Q_1 Q_2} \\ &\quad \cdot \left( \frac{1}{Q_1 + Q_2 + |\mu|} + \frac{\theta(Q_1 - |\mu|)}{Q_1 + Q_2 - |\mu|} + \frac{\theta(|\mu| - Q_1)}{Q_1 - Q_2 - |\mu|} \right).\end{aligned}\quad (8)$$

As a check, in the  $\mu = 0$  limit, we recover Eq.(65) in I, which is the gap equation for the case of  $T = 0$  and  $\mu = 0$ . Notice that Eq.(8) as well as Eq.(5) do not depend on the sign of  $\mu$ . For ease of writing, henceforth we drop the magnitude notation on  $|\mu|$  with the understanding that  $\mu$  stands for the nonnegative  $|\mu|$ .

In the small  $\mu$  limit where  $\mu \ll m_0$ , we may treat the chemical potential effects as a perturbation and write  $m^2(0, \mu) \simeq m_0^2 + \delta m_\mu^2$  with  $\delta m_\mu^2 \ll m_0^2$ . This allows us to obtain

$$\delta m_\mu^2 \simeq \frac{2I_2}{I_1} \mu^2, \quad (9)$$

where

$$\begin{aligned}I_1 &= \int_{-\infty}^{\infty} dq_3 \int_0^{\infty} d\hat{q}_\perp^2 \frac{e^{-\hat{q}_\perp^2}}{Q^2 Q_2 (Q + Q_2)} \left( \frac{1}{Q} + \frac{1}{Q + Q_2} \right), \\ I_2 &= \int_{-\infty}^{\infty} dq_3 \int_0^{\infty} d\hat{q}_\perp^2 \frac{e^{-\hat{q}_\perp^2}}{Q Q_2 (Q + Q_2)^3},\end{aligned}\quad (10)$$

and  $Q^2 \equiv q_3^2 + m_0^2$ . Note that  $I_1$  and  $I_2$  are the same integrals as defined in Eq.(67) of I. They are both finite and positive so that  $\delta m_\mu^2$  is positive.

In the large  $\mu$  limit where  $\mu \gg m_0$ , we may rewrite Eq.(8) as

$$1 \simeq -\frac{2\alpha}{\pi} |eH| \int_0^\infty d\hat{q}_\perp^2 e^{-\hat{q}_\perp^2} \left[ \int_0^{\sqrt{\mu^2 - m^2}} \frac{dq_3}{Q_2} \frac{1}{(\mu + Q_2)^2 - Q_1^2} \right. \\ \left. - \int_{\sqrt{\mu^2 - m^2}}^\infty \frac{dq_3}{Q_2} \frac{1 + \frac{Q_2}{Q_1}}{(Q_1 + Q_2)^2 - \mu^2} \right]. \quad (11)$$

Since both  $q_3$ -integrals are dominated by values of  $q_3$  near the respective lower limit of integration, it is clear that the first term in the square bracket is larger than the second term. Consequently the right hand side of the gap equation is negative and there is no solution for large  $\mu$ . This implies that there is a critical chemical potential above which chiral symmetry is restored. Indeed, this expectation is confirmed by the result of our numerical study discussed below.

Being unable to solve the gap equation, Eq.(8), analytically, we seek a numerical solution instead. It is convenient to introduce the following dimensionless variables:

$$\hat{q}_3 \equiv \frac{q_3}{\sqrt{2|eH|}}, \quad \hat{m}_\mu \equiv \frac{m(0, \mu)}{\sqrt{2|eH|}}, \quad \hat{\mu} \equiv \frac{\mu}{\sqrt{2|eH|}}, \quad \hat{Q}_{1,2} \equiv \frac{Q_{1,2}}{\sqrt{2|eH|}}. \quad (12)$$

In terms of these variables, Eq.(8) becomes

$$1 \simeq \frac{2\alpha}{\pi} I(\hat{m}_\mu, \hat{\mu}), \quad (13)$$

where

$$I(\hat{m}_\mu, \hat{\mu}) = \frac{1}{4} \int_0^\infty d\hat{q}_3 \int_0^\infty d\hat{q}_\perp^2 \frac{e^{-\hat{q}_\perp^2}}{\hat{Q}_1 \hat{Q}_2} \\ \cdot \left( \frac{1}{\hat{Q}_1 + \hat{Q}_2 + \hat{\mu}} + \frac{\theta(\hat{Q}_1 - \hat{\mu})}{\hat{Q}_1 + \hat{Q}_2 - \hat{\mu}} - \frac{\theta(\hat{\mu} - \hat{Q}_1)}{\hat{\mu} - \hat{Q}_1 + \hat{Q}_2} \right). \quad (14)$$

For various values of  $\hat{\mu}$  and  $\hat{m}_\mu$ , one can perform the double integration numerically. The result is shown in Fig. 1 where we have plotted  $I(\hat{m}_\mu, \hat{\mu})$  as a function of  $\hat{m}_\mu$  for five representative values of successively increasing  $\hat{\mu}$  from  $\hat{\mu} = 0$  to  $\hat{\mu} = 0.004243$ . The numerical solution for  $\hat{m}_\mu$  for each value of  $\hat{\mu}$  can be read off by equating  $I(\hat{m}_\mu, \hat{\mu})$  to

$\pi/2\alpha$ . For illustrative purpose, we have used  $\alpha = \pi/30$  in Fig. 1. Going from Fig. 1b to Fig. 1c, as  $\hat{\mu}$  increases, one finds two solutions for  $\hat{m}_\mu$  instead of one. As is clear from Fig. 1a,b,c, the requirement of continuity to the  $\hat{\mu} = 0$  solution selects the larger value of  $\hat{m}_\mu$  as the consistent solution [9]. Increasing  $\hat{\mu}$  to 0.004101, one finds again only one solution for  $\hat{m}_\mu$ , as shown in Fig. 1d. Further increase in  $\hat{\mu}$  results in no solution as indicated in Fig. 1e. We therefore conclude that the critical value of  $\hat{\mu}$  is 0.004101 (for  $\alpha = \pi/30$ ) above which chiral symmetry is restored.

In Fig. 2, the dimensionless dynamical fermion mass  $\hat{m}_\mu$  is plotted as a function of the dimensionless chemical potential  $\hat{\mu}$  for  $\alpha = \pi/30$ . We note that the phase transition across the critical chemical potential is of first order as the dynamical fermion mass has a discontinuity at the transition point. The order parameter also exhibits such a discontinuity. The chiral condensate at  $T = 0$  and  $\mu \neq 0$  can be obtained from Eq.(5) by noting that  $S_{0\mu} = \theta(\sqrt{p_3^2 + m_\mu^2} - \mu)$ , where  $m_\mu$  denotes  $m(0, \mu)$ . We find

$$\langle \bar{\psi} \psi \rangle_{0\mu} \simeq - \frac{|eH|}{\pi^2} m_\mu \left[ \theta(m_\mu - \mu) \int_0^{\sqrt{|eH|}} \frac{dp_3}{\sqrt{p_3^2 + m_\mu^2}} + \theta(\mu - m_\mu) \int_{\sqrt{\mu^2 - m_\mu^2}}^{\sqrt{|eH|}} \frac{dp_3}{\sqrt{p_3^2 + m_\mu^2}} \right]. \quad (15)$$

Since  $m_\mu = 0$  above the critical chemical potential and  $m_\mu > \mu$  for  $\mu < \mu_c$  (see Fig. 2), only the first integral on the right hand side of Eq.(15) contributes. The result is

$$\langle \bar{\psi} \psi \rangle_{0\mu} \simeq - \frac{|eH|}{2\pi^2} m_\mu \ln \left( \frac{|eH|}{m_\mu^2} \right). \quad (16)$$

Clearly, the result in Eq.(7) is recovered when  $\mu = 0$ . It is also apparent that the discontinuity in  $m_\mu$  is reflected as a discontinuity in  $\langle \bar{\psi} \psi \rangle_{0\mu}$  at the critical chemical potential.

One can numerically compute the critical chemical potential  $\hat{\mu}_c$  for different values of  $\alpha$ . The result, as depicted by the solid curve in Fig. 3, shows that  $\hat{\mu}_c$  increases with  $\alpha$ . This is an expected behavior because it requires a larger chemical potential to destabilize a more strongly coupled chiral condensate.

A closer examination of Fig. 1 shows that, for each value of  $\hat{\mu}$ ,  $I(\hat{m}_\mu, \hat{\mu})$  peaks at  $\hat{m}_\mu = \hat{\mu}$ . One can understand this feature qualitatively. For a given value of  $\hat{\mu}$ , let us

consider the integral  $I(\hat{m}_\mu, \hat{\mu})$  as a function of  $\hat{m}_\mu$ . For  $\hat{m}_\mu > \hat{\mu}$ , Eq.(14) becomes

$$I(\hat{m}_\mu, \hat{\mu}) = \frac{1}{4} \int_0^\infty d\hat{q}_3 \int_0^\infty d\hat{q}_\perp^2 \frac{e^{-\hat{q}_\perp^2}}{\sqrt{(\hat{q}_3^2 + \hat{m}_\mu^2)(\hat{q}_3^2 + \hat{q}_\perp^2)}} \cdot \left( \frac{1}{\sqrt{\hat{q}_3^2 + \hat{m}_\mu^2} + \hat{\mu} + \sqrt{\hat{q}_3^2 + \hat{q}_\perp^2}} + \frac{1}{\sqrt{\hat{q}_3^2 + \hat{m}_\mu^2} - \hat{\mu} + \sqrt{\hat{q}_3^2 + \hat{q}_\perp^2}} \right). \quad (17)$$

Clearly,  $I(\hat{m}_\mu, \hat{\mu})$  increases monotonically as  $\hat{m}_\mu$  is decreased; so in the region where  $\hat{m}_\mu > \hat{\mu}$ ,  $I(\hat{m}_\mu, \hat{\mu})$  reaches its maximum at  $\hat{m}_\mu = \hat{\mu}$ . For  $\hat{m}_\mu < \hat{\mu}$ , we may examine the slope

$$\begin{aligned} \frac{\partial I}{\partial \hat{m}_\mu} = & \hat{m}_\mu \int_0^\infty d\hat{q}_3 \int_0^\infty d\hat{q}_\perp^2 \frac{e^{-\hat{q}_\perp^2}}{\hat{Q}_2} \left\{ \frac{1}{\hat{Q}_2} \frac{1}{2\hat{\mu}\sqrt{\hat{\mu}^2 - \hat{m}_\mu^2}} \delta(\hat{q}_3 - \sqrt{\hat{\mu}^2 - \hat{m}_\mu^2}) \right. \\ & - \frac{\theta(\hat{\mu} - \hat{Q}_1)}{[(\hat{\mu} + \hat{Q}_2)^2 - \hat{Q}_1^2]^2} \\ & \left. - \frac{\theta(\hat{Q}_1 - \hat{\mu})}{[(\hat{Q}_1 + \hat{Q}_2)^2 - \hat{\mu}^2]^2} \left( 1 + \frac{\hat{Q}_2}{2\hat{Q}_1} \left[ \left( 2 + \frac{\hat{Q}_2}{\hat{Q}_1} \right)^2 + \left( 1 - \frac{\hat{\mu}^2}{\hat{Q}_1^2} \right) \right] \right) \right\}. \end{aligned} \quad (18)$$

Note that it is zero at  $\hat{m}_\mu = 0$  and goes to infinity as  $\hat{m}_\mu$  approaches  $\hat{\mu}$ . Furthermore,  $\frac{1}{\hat{m}_\mu} \frac{\partial I}{\partial \hat{m}_\mu}$  is positive at  $\hat{m}_\mu = 0$  and the positive term in the integrand (the term proportional to the  $\delta$ -function) increases with increasing  $\hat{m}_\mu$  while all the negative terms decrease in magnitude. In other words, the slope is always positive for  $\hat{m}_\mu < \hat{\mu}$ . Hence, for fixed  $\hat{\mu}$ ,  $I(\hat{m}_\mu, \hat{\mu})$  is a monotonically increasing function of  $\hat{m}_\mu$  in the region  $\hat{m}_\mu < \hat{\mu}$ . The discontinuity of the slope at  $\hat{m}_\mu = \hat{\mu}$  indicates that  $I(\hat{m}_\mu, \hat{\mu})$  should peak sharply there, as we see from Fig. 1. We shall exploit this fact to estimate analytically the critical chemical potential.

As the chemical potential reaches  $\hat{\mu}_c$ ,  $I(\hat{m}_\mu, \hat{\mu}_c)$  peaks at  $\hat{m}_\mu = \hat{\mu}_c$  and  $I(\hat{\mu}_c, \hat{\mu}_c) = \pi/2\alpha$  satisfies the gap equation, Eq.(13). This implies that

$$\hat{m}_\mu^2(\hat{\mu} = \hat{\mu}_c) = \hat{\mu}_c^2. \quad (19)$$

Adopting the perturbative result in Eq.(9), we find

$$\mu_c \simeq \frac{m_0}{\sqrt{1 - \frac{2I_2}{I_1}}}. \quad (20)$$

This estimate of  $\mu_c$  is shown as the dotted curve in Fig. 3 where the approximate analytical solution for  $m_0$  (see Eq.(53) in I) has been used. The good agreement with the exact numerical result (solid curve in Fig. 3) indicates that the analytical estimate of the critical chemical potential is quite robust for small values of  $\alpha$ .

As noted above, the phase transition across the critical chemical potential is of first order. In I where we studied chiral symmetry breaking in an external magnetic field at nonzero temperature but with zero chemical potential, we showed that the chiral symmetry is restored above a critical temperature  $T_c$ . In the remainder of this paper, we would like to examine this phase transition across  $T_c$  in greater detail. With the introduction of the dimensionless temperature and dynamical fermion thermal mass:

$$\hat{T} \equiv \frac{T}{\sqrt{2|eH|}}, \quad \hat{m}_T \equiv \frac{m(T, 0)}{\sqrt{2|eH|}}, \quad (21)$$

the finite temperature gap equation can be obtained by setting  $\mu = 0$  in Eq.(3):

$$1 \simeq \frac{2\alpha}{\pi} J(\hat{m}_T, \hat{T}), \quad (22)$$

where

$$\begin{aligned} J(\hat{m}_T, \hat{T}) = & \frac{1}{2} \int_0^\infty d\hat{q}_3 \int_0^\infty d\hat{q}_\perp^2 \frac{e^{-\hat{q}_\perp^2}}{\sqrt{(\hat{q}_3^2 + \hat{m}_T^2)(\hat{q}_3^2 + \hat{q}_\perp^2)}} \\ & \cdot \left[ \left( \frac{1}{1 - e^{-\frac{\sqrt{\hat{q}_3^2 + \hat{q}_\perp^2}}{\hat{T}}}} + \frac{1}{1 + e^{-\frac{\sqrt{\hat{q}_3^2 + \hat{m}_T^2}}{\hat{T}}}} - 1 \right) \frac{\sqrt{\hat{q}_3^2 + \hat{m}_T^2} + \sqrt{\hat{q}_3^2 + \hat{q}_\perp^2}}{(\sqrt{\hat{q}_3^2 + \hat{m}_T^2} + \sqrt{\hat{q}_3^2 + \hat{q}_\perp^2})^2 + \pi^2 \hat{T}^2} \right. \\ & \left. + \left( \frac{1}{1 - e^{-\frac{\sqrt{\hat{q}_3^2 + \hat{q}_\perp^2}}{\hat{T}}}} - \frac{1}{1 + e^{-\frac{\sqrt{\hat{q}_3^2 + \hat{m}_T^2}}{\hat{T}}}} \right) \frac{\sqrt{\hat{q}_3^2 + \hat{m}_T^2} - \sqrt{\hat{q}_3^2 + \hat{q}_\perp^2}}{(\sqrt{\hat{q}_3^2 + \hat{m}_T^2} - \sqrt{\hat{q}_3^2 + \hat{q}_\perp^2})^2 + \pi^2 \hat{T}^2} \right] \end{aligned} \quad (23)$$

We have solved the above equation numerically. The result is shown in Fig. 4 where, for illustrative purpose, we have again used  $\alpha = \pi/30$ . The critical temperature at which the dynamical fermion mass vanishes is  $\hat{T}_c \approx 0.00205$  for this value of  $\alpha$ . As shown in Fig. 4, starting at  $\hat{T} = \hat{T}_c$ ,  $\hat{m}_T$  increases as  $\hat{T}$  decreases and it remains zero as  $\hat{T}$  increases indicating that the corresponding phase transition is of second order.

To find out how the dynamical fermion mass varies with temperature near (and below)  $\hat{T}_c$ , we expand  $J(\hat{m}_T, \hat{T})$  around  $\hat{m}_T^2 = 0$  and  $\hat{T} = \hat{T}_c$  so that for small  $\hat{T} - \hat{T}_c$  and small  $\hat{m}_T^2$ , Eq.(22) takes the form

$$1 \simeq \frac{2\alpha}{\pi} \left[ J(0, \hat{T}_c) + \frac{\partial J(0, \hat{T}_c)}{\partial \hat{T}} (\hat{T} - \hat{T}_c) + \frac{\partial J(0, \hat{T}_c)}{\partial \hat{m}_T^2} \hat{m}_T^2 \right]. \quad (24)$$

It can be shown both analytically and numerically that  $\frac{\partial J(0, \hat{T}_c)}{\partial \hat{T}}$  and  $\frac{\partial J(0, \hat{T}_c)}{\partial \hat{m}_T^2}$  are finite and negative. We can understand qualitatively why these two partial derivatives must have the same sign. According to the result in Fig. 4, increasing the temperature reduces the dynamical fermion thermal mass. It follows that raising the temperature must have the opposite effect on  $J(\hat{m}_T, \hat{T})$  as lowering the fermion thermal mass in order that the gap equation, Eq.(22), remains satisfied. Since  $\hat{m}_T^2 = 0$  for  $\hat{T} = \hat{T}_c$  solves the gap equation, we obtain from Eq.(24) that

$$0 = -\frac{\partial J(0, \hat{T}_c)}{\partial \hat{T}} \hat{T}_c \left( 1 - \frac{\hat{T}}{\hat{T}_c} \right) + \frac{\partial J(0, \hat{T}_c)}{\partial \hat{m}_T^2} \hat{m}_T^2, \quad (25)$$

which indicates that  $\hat{m}_T$  has the behavior

$$\hat{m}_T \sim \left( 1 - \frac{T}{T_c} \right)^{\frac{1}{2}} \quad (26)$$

as  $T$  approaches  $T_c$  from below. This translates into a similar behavior for the order parameter of this phase transition.

The chiral condensate at nonzero temperature and zero chemical potential can be gleaned from Eq.(5) to be

$$\begin{aligned} \langle \bar{\psi} \psi \rangle_{T0} &\simeq -\frac{|eH|}{\pi^2} m_T \int_0^{\sqrt{|eH|}} \frac{dp_3}{\sqrt{p_3^2 + m_T^2}} \tanh \left( \frac{\sqrt{p_3^2 + m_T^2}}{2T} \right) \\ &\simeq -\frac{|eH|}{2\pi^2} m_T \ln \left( \frac{|eH|}{m_T^2} \right), \end{aligned} \quad (27)$$

where  $m_T$  denotes  $m(T, 0)$  and the last result is obtained by noting that the integral is dominated by large values of  $p_3$  for which the hyperbolic tangent function in the integrand is approximately 1 (for  $T < T_c$ ). Eq.(26) and Eq.(27) show that

$$\langle \bar{\psi} \psi \rangle_{T0} \sim |eH|^{\frac{3}{2}} \left(1 - \frac{T}{T_c}\right)^{\frac{1}{2}} \ln \left(1 - \frac{T}{T_c}\right)^{\frac{1}{2}} \quad (28)$$

as  $T \rightarrow T_c^-$ .

To summarize, we have considered the separate effects of a chemical potential and temperature on the chiral symmetry breaking induced by an external uniform magnetic field in quenched, ladder QED. We have done so in order to highlight the effects of each. Of course, it is useful and interesting to consider their combined effects. Work along this direction is in progress.

## ACKNOWLEDGEMENTS

This work was supported in part by the U.S. Department of Energy under Grants No. DE-FG02-84ER40163 and DE-FG05-85ER-40219 Task A. Part of this work was done recently when C.N.L. was visiting the Institute of Physics at the Academia Sinica in Taipei. He thanks H.-L. Yu and other institute members there for their hospitality. He also thanks the National Science Council of the R.O.C. for support under Grant NSC86-2811-M-001-065R.

## REFERENCES

- [1] Y.J. Ng and Y. Kikuchi, in *Vacuum Structure in Intense Fields*, eds. H. M. Fried and B. Müller (Plenum, New York, 1991); Y.J. Ng, in *Tests of Fundamental Laws in Physics*, eds. O. Fackler and J. Tran Thanh Van (Editions Frontiers, 33 Gif-sur-Yvette Cedex, 1989).
- [2] V. P. Gusynin, V. A. Miransky, and I. A. Shovkovy, Phys. Rev. D **52**, 4747 (1995); Nucl. Phys. **B462**, 249 (1996). See also D. K. Hong, Y. Kim and S.-J. Sin, Phys. Rev. D **54**, 7879 (1996).
- [3] C. N. Leung, Y. J. Ng, and A. W. Ackley, Phys. Rev. D **54**, 4181 (1996).
- [4] D.-S. Lee, C. N. Leung and Y. J. Ng, Phys. Rev. D **55**, 6504 (1997).
- [5] V. P. Gusynin and I. A. Shovkovy, Phys. Rev. D **56**, 5251 (1997).
- [6] See, e.g., J. Kapusta, *Finite-Temperature Field Theory* (Cambridge University Press, Cambridge, England, 1989).
- [7] See Ref. 9 in Ref. [4].
- [8] See Eq.(64); there is a typographical mistake:  $e^{-\sqrt{\frac{Q_{1,2}}{T}}}$  should be replaced by  $e^{-\frac{\sqrt{Q_{1,2}}}{T}}$ .
- [9] In fact, one has to compute the corresponding effective potential to see if these solutions are stable and if the other branch of solutions corresponding to smaller values of  $\hat{m}_\mu$  are unstable. Here we content ourselves by simply applying the continuity criterion.

## FIGURE CAPTIONS

**Fig. 1a:**  $I(\hat{m}_\mu, \hat{\mu})$  vs.  $\hat{m}_\mu$  for  $\hat{\mu} = 0$ .  $I(\hat{m}_\mu, \hat{\mu})$  peaks at  $\hat{m}_\mu = \hat{\mu} = 0$ . The solution to the gap equation is at  $\hat{m}_\mu = 0.003790$  for  $\alpha = \pi/30$ .

**Fig. 1b:**  $I(\hat{m}_\mu, \hat{\mu})$  vs.  $\hat{m}_\mu$  for  $\hat{\mu} = 0.001414$ .  $I(\hat{m}_\mu, \hat{\mu})$  peaks at  $\hat{m}_\mu = \hat{\mu} = 0.001414$ . The solution to the gap equation is at  $\hat{m}_\mu = 0.003817$  for  $\alpha = \pi/30$ .

**Fig. 1c:**  $I(\hat{m}_\mu, \hat{\mu})$  vs.  $\hat{m}_\mu$  for  $\hat{\mu} = 0.002828$ .  $I(\hat{m}_\mu, \hat{\mu})$  peaks at  $\hat{m}_\mu = \hat{\mu} = 0.002828$ . Note that there are two possible solutions to the gap equation at  $\hat{m}_\mu = 0.002715$  and  $0.003889$  for  $\alpha = \pi/30$ .

**Fig. 1d:**  $I(\hat{m}_\mu, \hat{\mu})$  vs.  $\hat{m}_\mu$  for  $\hat{\mu} = 0.004101$ .  $I(\hat{m}_\mu, \hat{\mu})$  peaks at  $\hat{m}_\mu = \hat{\mu} = 0.004101$ . There is one solution to the gap equation at  $\hat{m}_\mu = \hat{\mu} = 0.004101$  for  $\alpha = \pi/30$ .

**Fig. 1e:**  $I(\hat{m}_\mu, \hat{\mu})$  vs.  $\hat{m}_\mu$  for  $\hat{\mu} = 0.004243$ .  $I(\hat{m}_\mu, \hat{\mu})$  peaks at  $\hat{m}_\mu = \hat{\mu} = 0.004243$ . There is no solution to the gap equation for  $\alpha = \pi/30$ .

**Fig. 2:** The dynamical fermion mass  $m_\mu$  as a function of the chemical potential  $\mu$  (both measured in units of  $\sqrt{2|eH|}$ ) for  $\alpha = \pi/30$ . The corresponding dimensionless critical chemical potential  $\hat{\mu}_c$  is equal to 0.004101.

**Fig. 3:** The critical chemical potential (measured in units of  $\sqrt{2|eH|}$ ) as a function of the gauge coupling  $\alpha$ . Solid curve: from exact numerical calculations. Dotted curve: from the estimate in Eq.(20).

**Fig. 4:** The dynamical fermion thermal mass  $m_T$  as a function of the temperature (both measured in units of  $\sqrt{2|eH|}$ ) for  $\alpha = \pi/30$ .

Fig. 1a

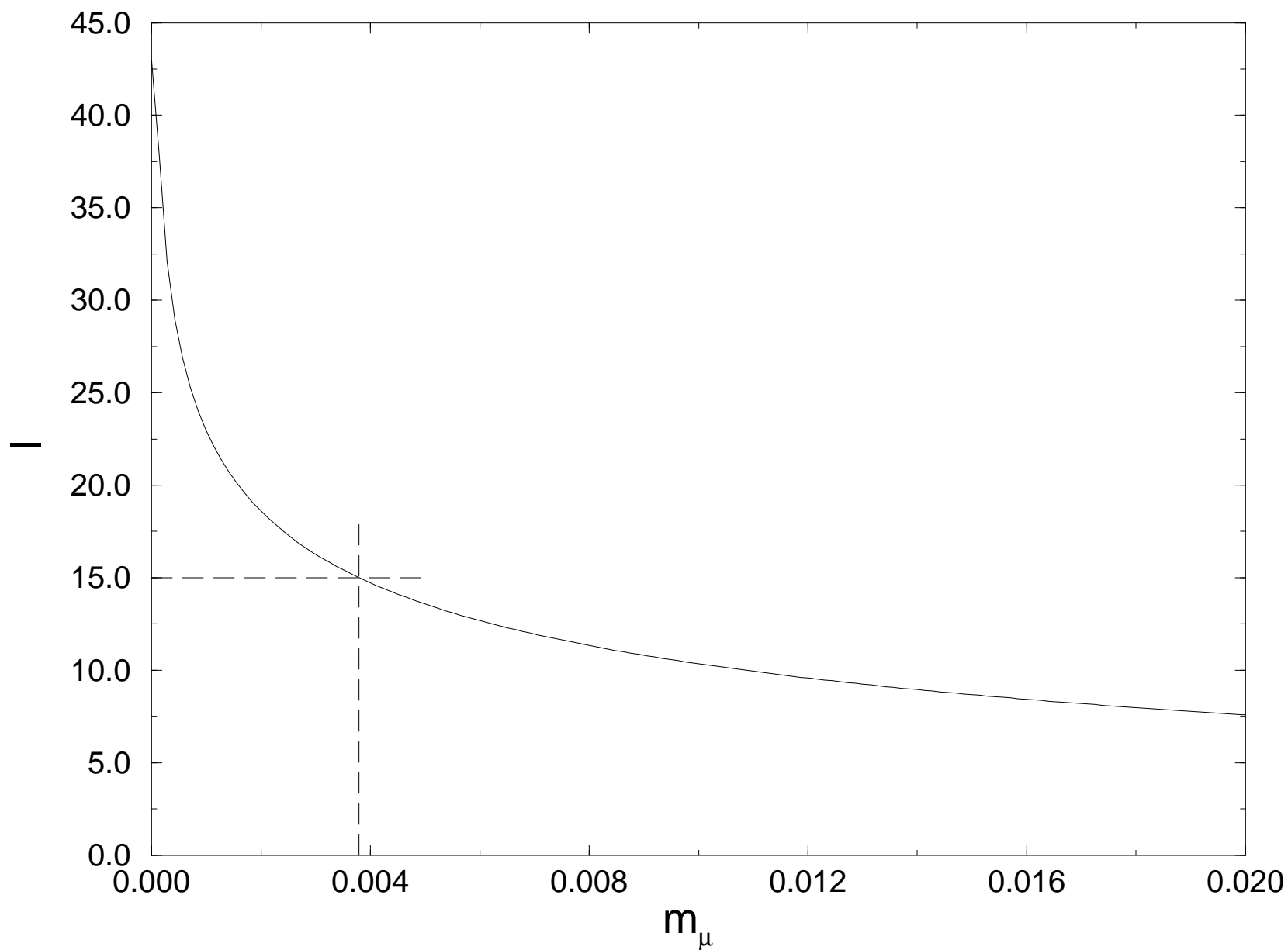


Fig. 1b

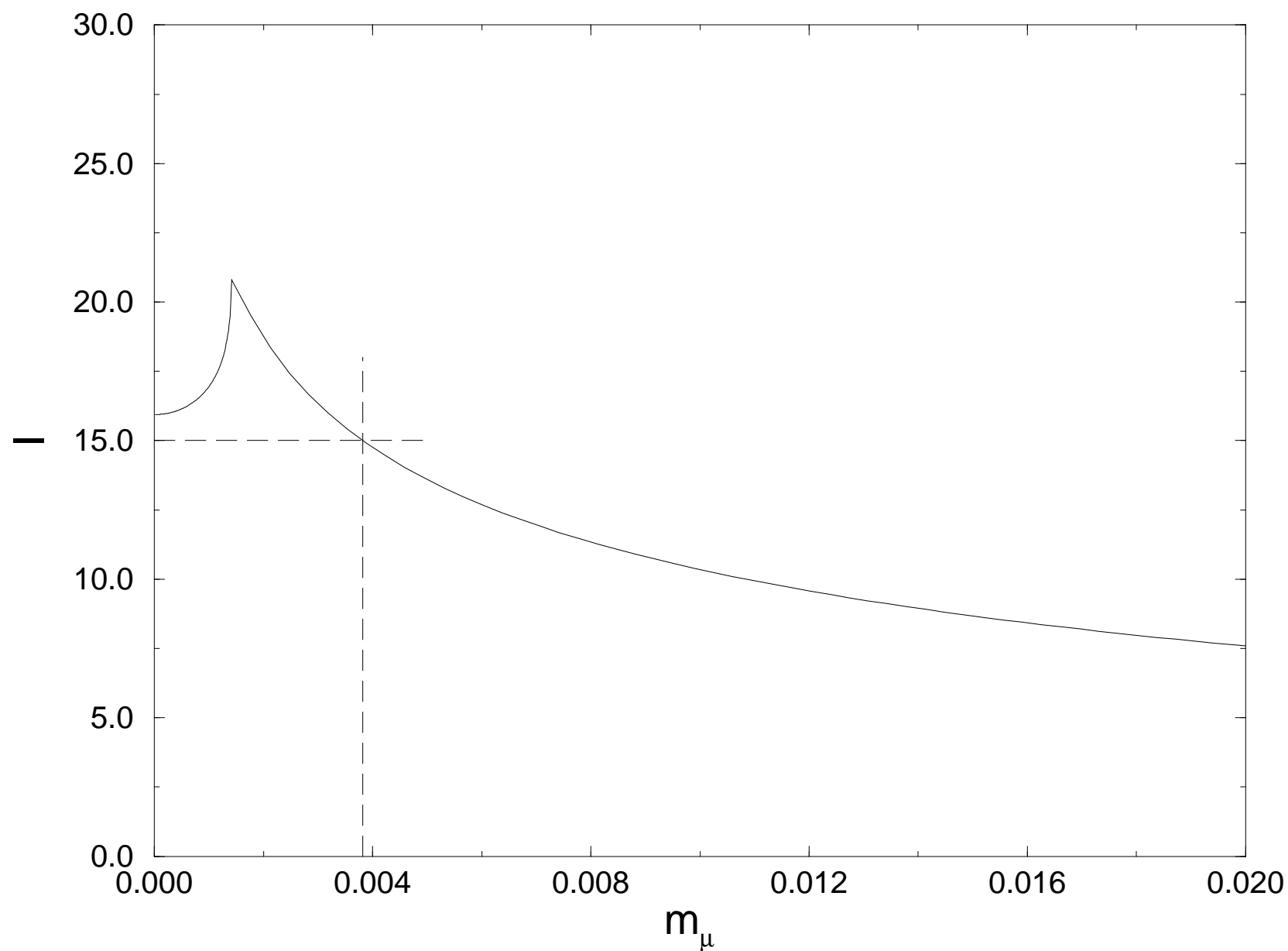


Fig. 1c

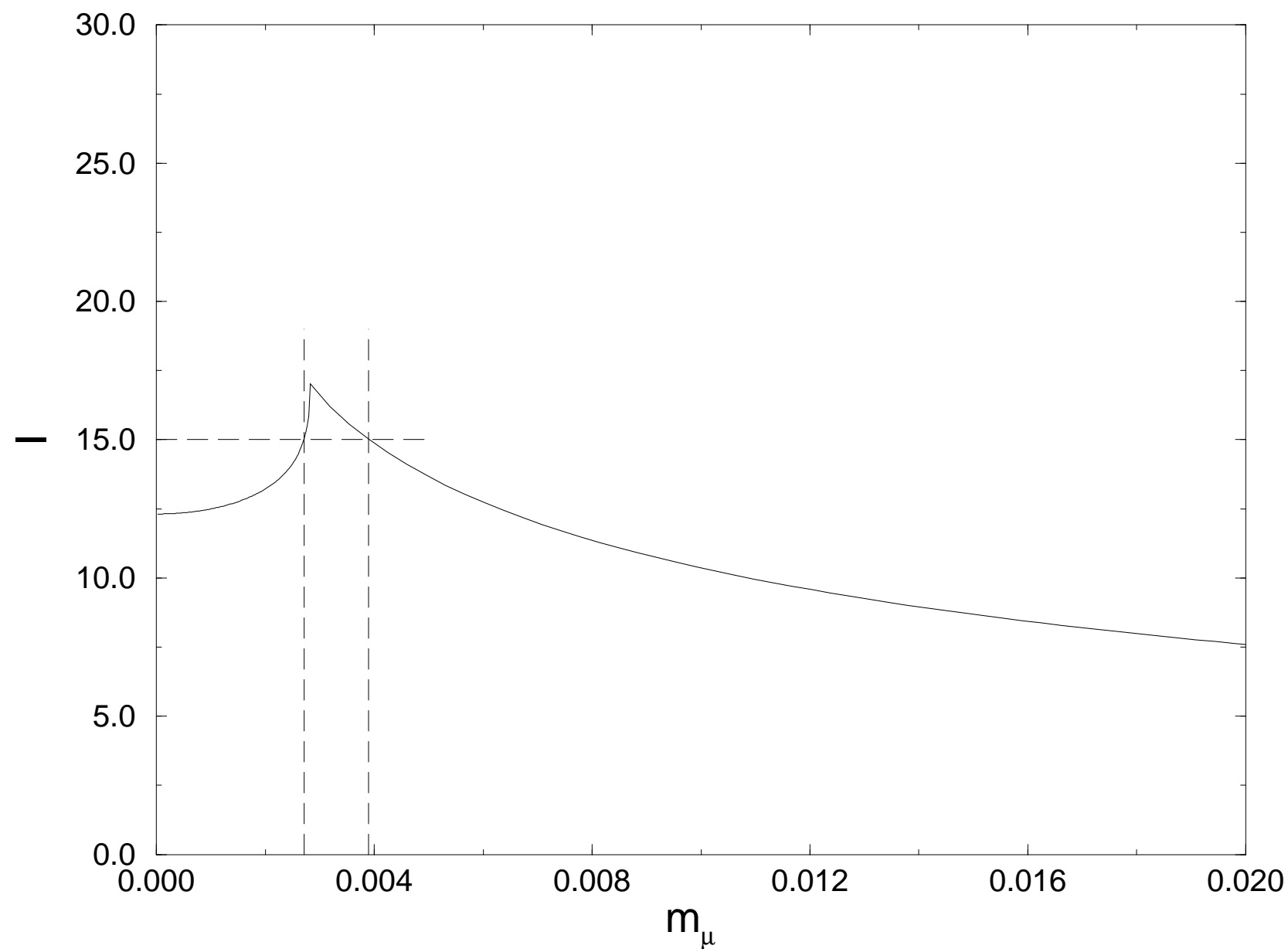


Fig. 1d

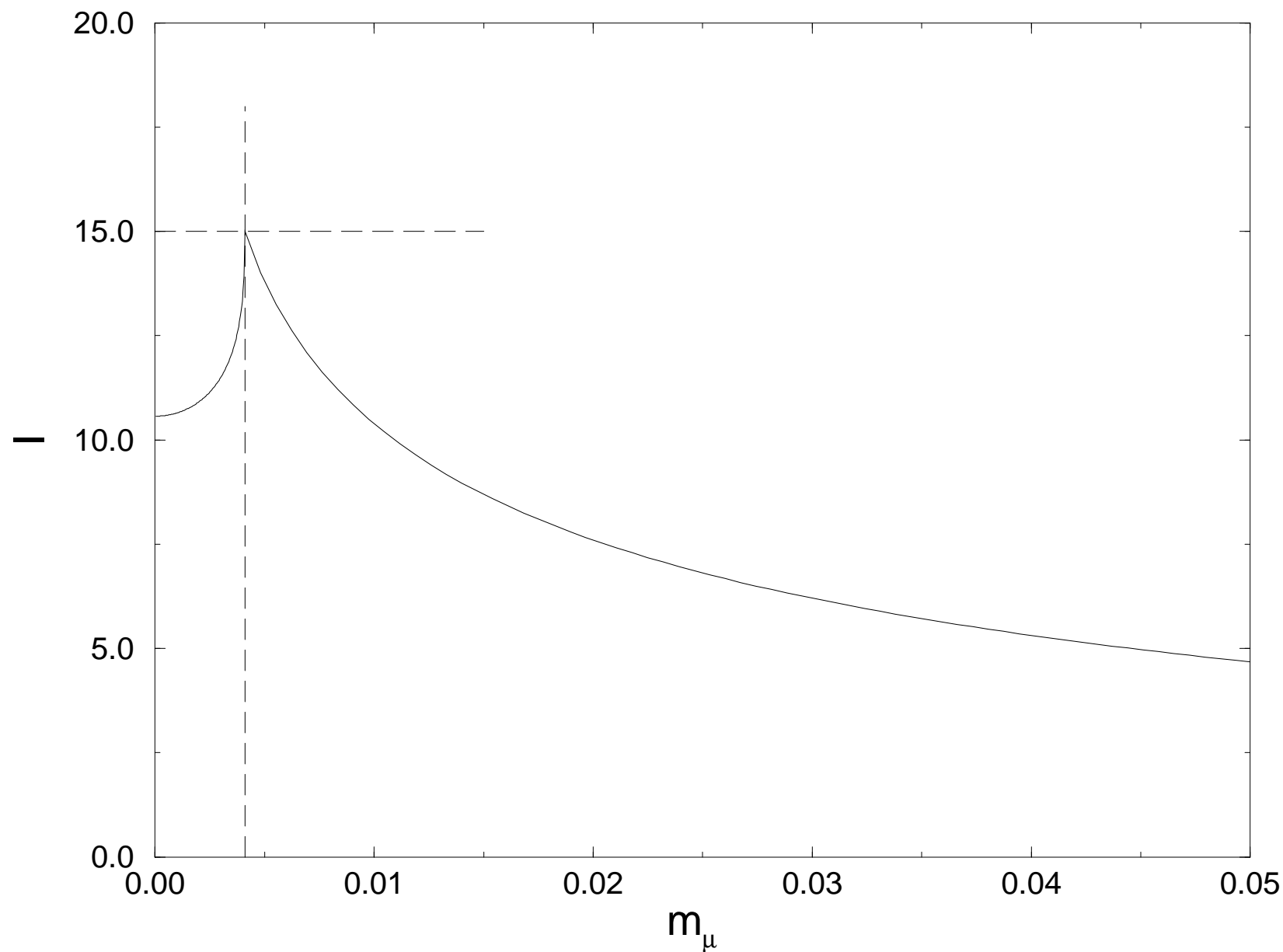


Fig. 1e

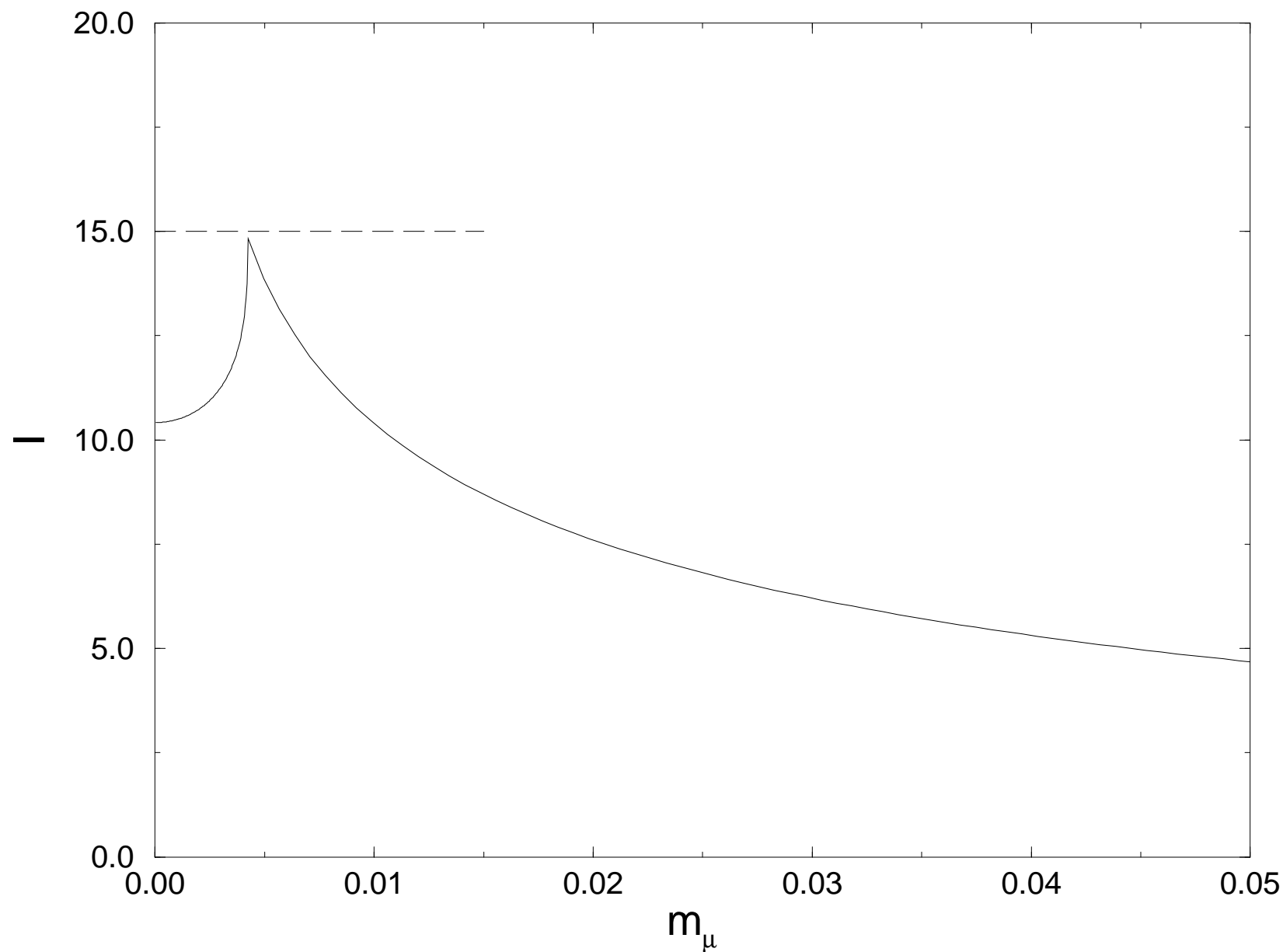


Fig. 2

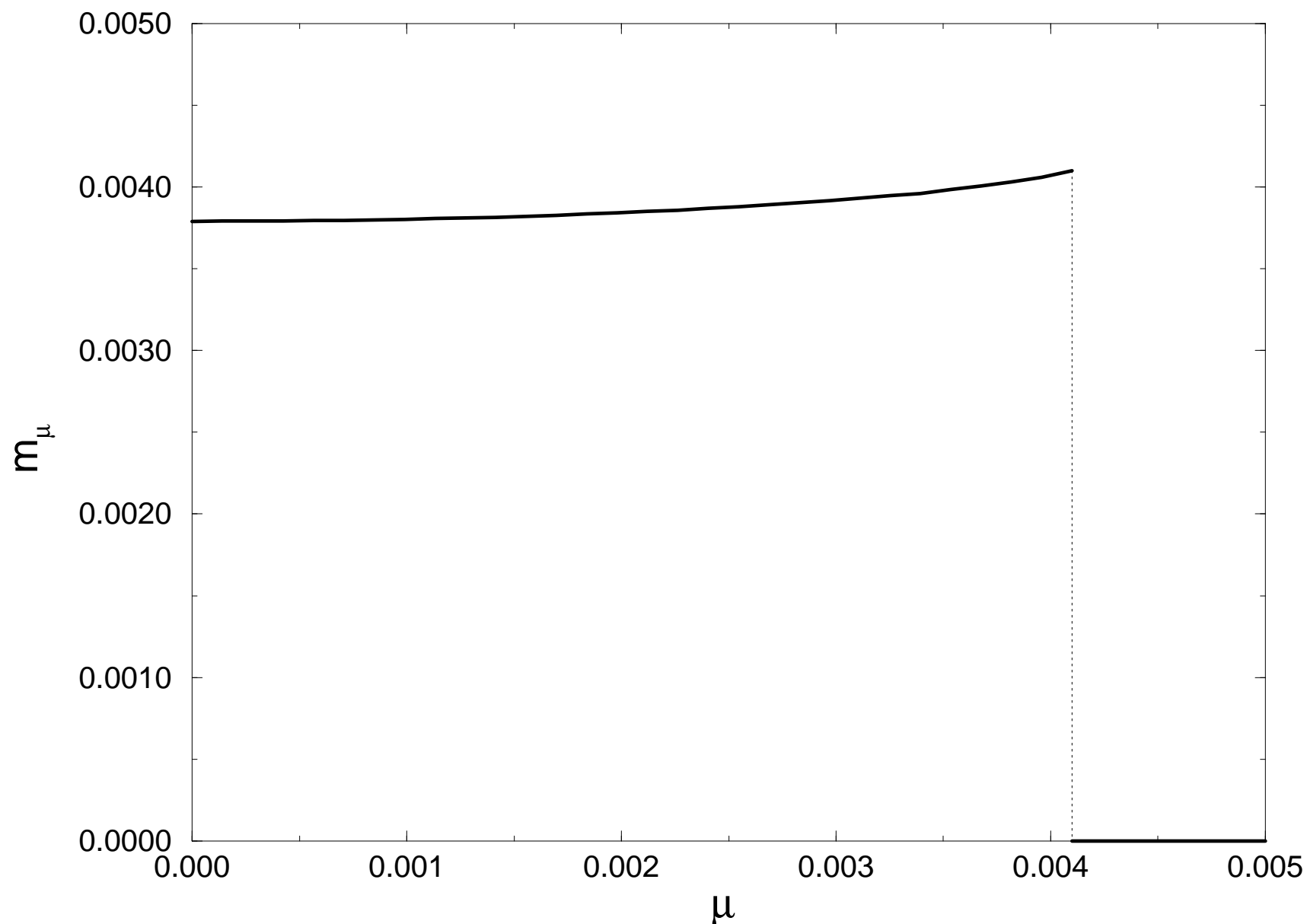


Fig. 3

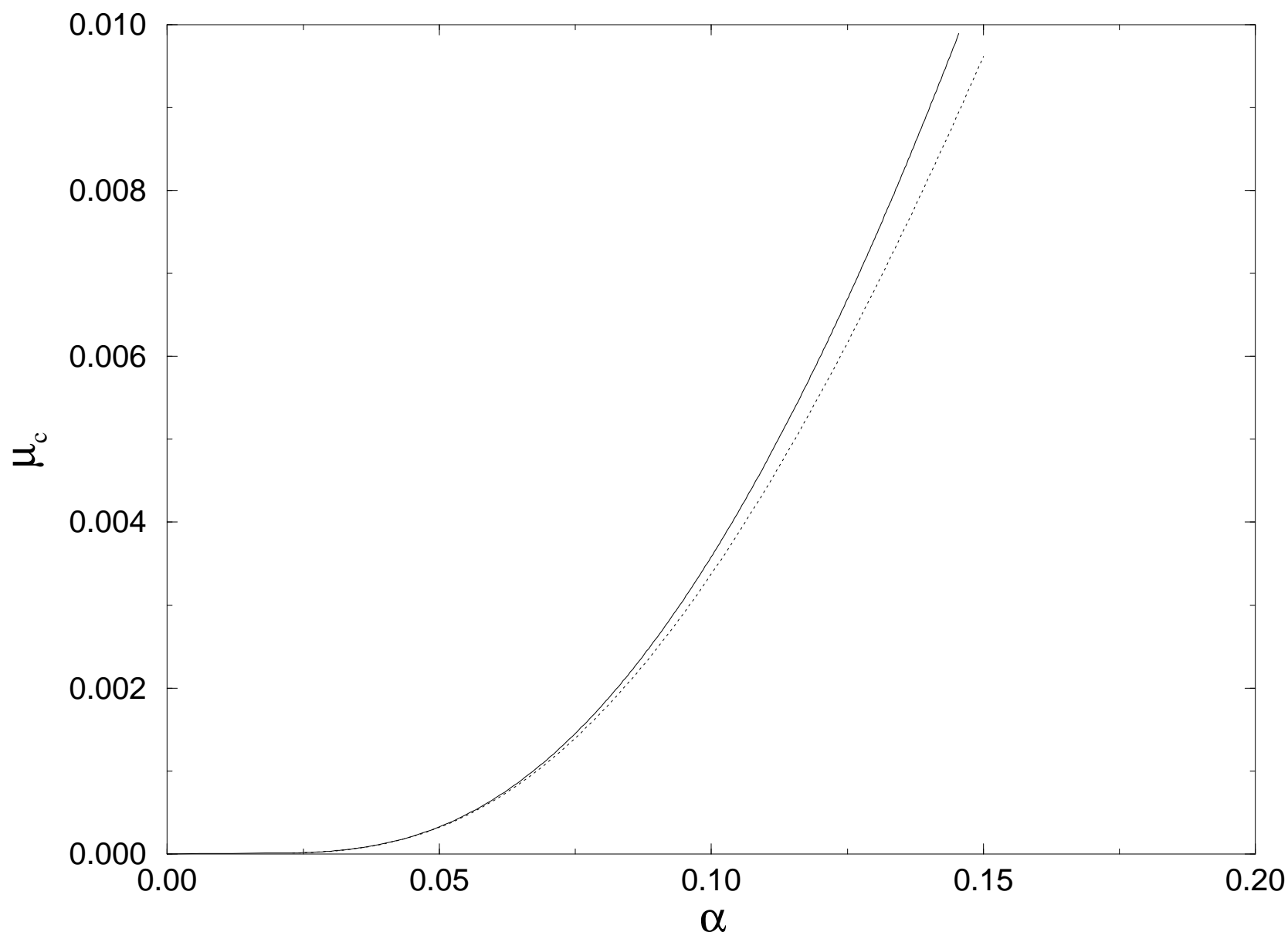


Fig. 4

